

pubs.acs.org/macroletters Letter

## **RAFT Step-Growth Polymerization of Diacrylates**

Noel E. Archer, Parker T. Boeck, Yasmin Ajirniar, Joji Tanaka,\* and Wei You\*



Cite This: ACS Macro Lett. 2022, 11, 1079–1084



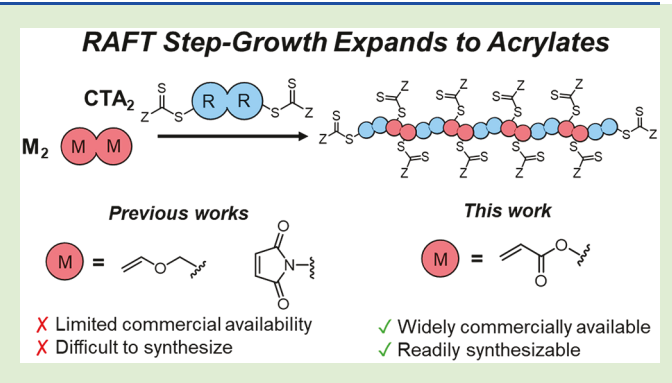
**ACCESS** 

III Metrics & More

Article Recommendations

Supporting Information

ABSTRACT: RAFT step-growth polymerization was previously demonstrated with monomers that bear low rate of homopropagation to favor the chain transfer process; by contrast, acrylates are known to be fast homopropagating monomers, thereby posing serious challenges for RAFT step-growth. Here, we identified a chain transfer agent (CTA) that rapidly yields single unit monomer inserted (SUMI) CTA adducts with a model acrylate monomer. Using a bifunctional reagent of this CTA, we successfully demonstrated RAFT step-growth polymerization with diacrylates, yielding linear polymer backbones. Furthermore, we achieved inclusion of functionality (i.e., disulfide) into RAFT step-growth polymer via a disulfide incorporated bifunctional CTA. Grafting from this backbone resulted in molecular brush polymers with



cleavable functionality in each repeat unit of the backbone, allowing selective degradation to afford well-defined unimolecular species of two polymeric side chains. Given the wide selection of commercially available diacrylates, RAFT step-growth polymerization of diacrylates will further enable facile synthesis of complex architectures with modular backbones.

Reversible-addition—fragmentation chain transfer (RAFT)<sup>1</sup> polymerization of vinyl monomers is a robust and user-friendly technique that can be used to create complex polymer structures.<sup>2–5</sup> However, the chain-growth nature of RAFT polymerization usually dictates an all-carbon backbone with functional groups—if desired—on the pendant side chain or at the termini of the backbone.<sup>6</sup> By contrast, step-growth polymerization—which proceeds by joining two end groups of monomers together—allows the possibility to incorporate various functionalities along the polymer backbone. However, traditional step-growth polymerization requires demanding reaction conditions and offers limited control over polymer architectures.<sup>7</sup>

Depending on the relative CTA reactivity and monomer, the initial stages of RAFT polymerization can quantitatively yield a single unit monomer inserted (SUMI) CTA adduct prior to further propagation.<sup>8</sup> This important insight was first investigated by McLeary and Klumperman, 9-11 and independently confirmed by Chen and Ghiggino with stoichiometric ratio of monomer to CTA. 12,13 Taking advantage of the RAFT-SUMI cycle, we recently reported *RAFT step-growth polymerization* by using bifunctional reagents bearing CTA and monomer functionalities that yield high SUMI-CTA adducts. RAFT step-growth polymerization synergistically combines the desirable features of both RAFT (functional group tolerance and user-friendly nature) and step-growth (functional backbone). 14,15 Shortly after, Li and Zhu independently reported a catalyst-free, photomediated RAFT step-growth. 16

Figure 1A outlines the proposed mechanism of RAFT stepgrowth polymerization. Specifically, the R $^{\bullet}$  (fragmented CTA end group species) adds to the monomer end group (M) to generate the R-M $^{\bullet}$  ( $k_{\rm i}$ ), which can react with R-group bearing CTA species ( $k_{\rm add}$ ) to form the chain transfer intermediate adduct. Fragmentation of this intermediate ( $k_{\rm frag}$ ) regenerates the R $^{\bullet}$  and concurrently appends CTA to the backbone repeat unit. However, branching would occur if R-M $^{\bullet}$  reacts with additional monomer species, which is dictated by the homopolymerization rate of the monomer ( $k_{\rm p}$ ). To limit this occurrence, monomers with low  $k_{\rm p}$  were chosen (maleimides and vinyl ether) in previous reports to promote chain transfer cycle. <sup>14–16</sup> To date, more reactive monomers such as acrylates that bear high  $k_{\rm p}$  have never been explored for RAFT stepgrowth polymerization.

Interestingly, McLeary and Klumperman earlier showed that methyl acrylate (in much greater excess than CTA) would selectively react with CTAs until almost all CTAs were converted into the SUMI-CTA (n = 1) adduct before forming multiple monomer insertion adducts  $(n \ge 2)$ ;<sup>8</sup> this was ascribed by Moad et al. to the significant chain transfer constant of CTAs, which describes the likelihood of  $M^{\bullet}$  species

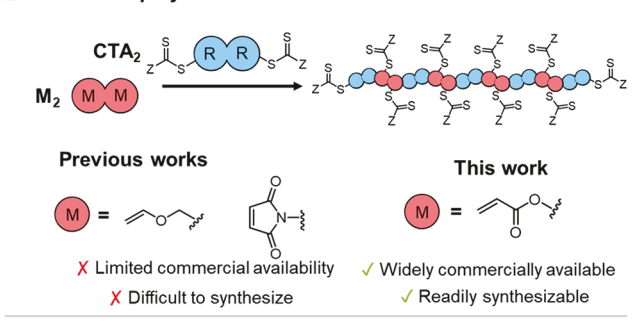
Received: August 10, 2022 Accepted: August 17, 2022 Published: August 19, 2022





# 

#### B General polymerization scheme



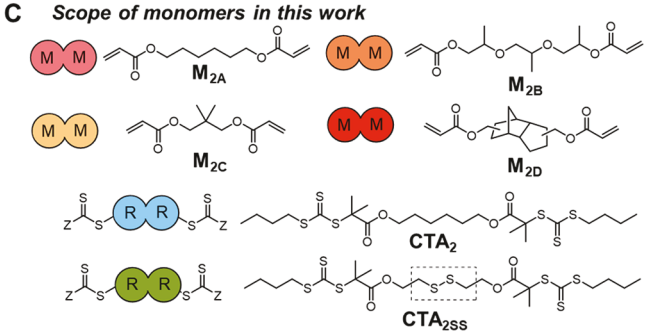


**Figure 1.** (A) Proposed mechanistic cycle for RAFT step-growth polymerization. Boxed is the undesirable homopolymerization. (B) General structure of  $A_2$ - $B_2$  RAFT step growth polymerization. (C) Structure of monomers.

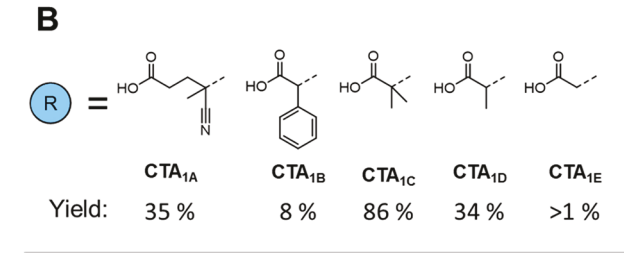
undergoing chain transfer over homopropagation.  $^{17,18}$  We hypothesized that RAFT step-growth polymerization could be achieved with acrylates if a suitable CTA was identified to ensure  $k_{\rm add}$  outweighs  $k_{\rm p}$ .

Here we show A<sub>2</sub> + B<sub>2</sub> RAFT step-growth with diacrylic monomers, which are a class of monomers that are not only synthetically easy to prepare but also widely commercially available and often inexpensive (Figure 1B). In addition, previously, incorporation of functional groups into the polymer backbone was demonstrated though the bifunctional *monomer*, and here we show the incorporation of a degradable disulfide moiety through the bifunctional *CTA unit* (Figure 1C). Finally, RAFT step-growth polymers were used to prepare molecular brush polymers, and cleavage of the brush backbone was demonstrated, forming narrow molecular weight species of two linked polymer side chains.

The key to a successful RAFT step-growth is to identify suitable pairing of a CTA functionality with the monomer (acrylate in this case); we followed the same protocol in our earlier work<sup>14</sup> to screen various CTAs that could yield selective SUMI-CTA adducts under stoichiometrically balanced con-

ditions  $(r = [M]_0/[CTA]_0 = 1)$  (Figure 2A). We decided to employ trithiocarbonate based CTAs to match the Z-group

$$\begin{array}{c} A \\ \hline M \\ = \\ \hline \\ M_1 \\ \hline \\ R \\ S \\ CTA_1 \end{array} \begin{array}{c} AIBN \\ \hline \\ dioxane \\ 70 \ ^{\circ}C \\ \hline \\ M_1\text{-CTA}_1 (SUMI\text{-CTA} adduct) \end{array}$$



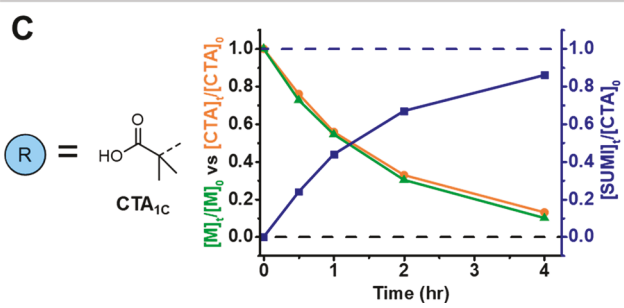


**Figure 2.** General conditions for screening of CTA for RAFT step-growth of acrylic monomer.

reactivity with monomer, to ensure rapid chain transfer while limiting the RAFT retardation. We used butyl acrylate (BA) as a model acrylic monomer at 2 M concentration ([BA] $_0$  = 2 M) in dioxane, and we initiated the RAFT SUMI process with AIBN as the initiator ([AIBN] $_0$  = 50 mM) at 70 °C, leaving the reaction for 4 h unless stated otherwise.

Initially, 4-cyano-4-(((dodecylthio)carbonothioyl)thio) pentanoic acid (CDTPA, CTA<sub>1A</sub>) was examined (Figure 2B, Figure S4), which had been reported to show high RAFT-SUMI yields under stochiometric conditions with styrene and acrylamidic monomers by Moad. 20,21 However, limited yields (35%, Figure 2B) were obtained after 8 h (Figure S3). As the fragmentation of CTA<sub>1A</sub> generates cyano-stabilized tertiary radical  $(R \cdot)$ , we reason the addition to acrylic monomer to form carbonyl ester stabilized secondary radical is rate limiting, as suggested by Moad.  $^{20,21}$  Interestingly, CTA<sub>1C</sub>, which was used in our previous RAFT step-growth report, 14 was found to have the highest SUMI CTA adduct yields (86%) as well as equal consumption of monomer and CTA (Figure 1, Figures S3, S6). We also explored CTA<sub>1B</sub> which bears intermediate reactivity between  ${\rm CTA_{1A}}$  and  ${\rm CTA_{1C}}$  in the literature (Figure S5);<sup>22</sup> however, it was found to generate even lower yields (7.6%) than the former two CTAs (Figure 1, Figure S3). Additionally, CTA<sub>1D</sub> with a less-stabilized radical after fragmentation (Figure 1, Figure S7) resulted in a higher consumption of the monomer than the CTA (Figure S3), indicative of multiple monomer addition, as the products of fragmentation do not drive the chain transfer equilibrium. Lastly, CTA<sub>1E</sub> that bears primary radical upon fragmentation

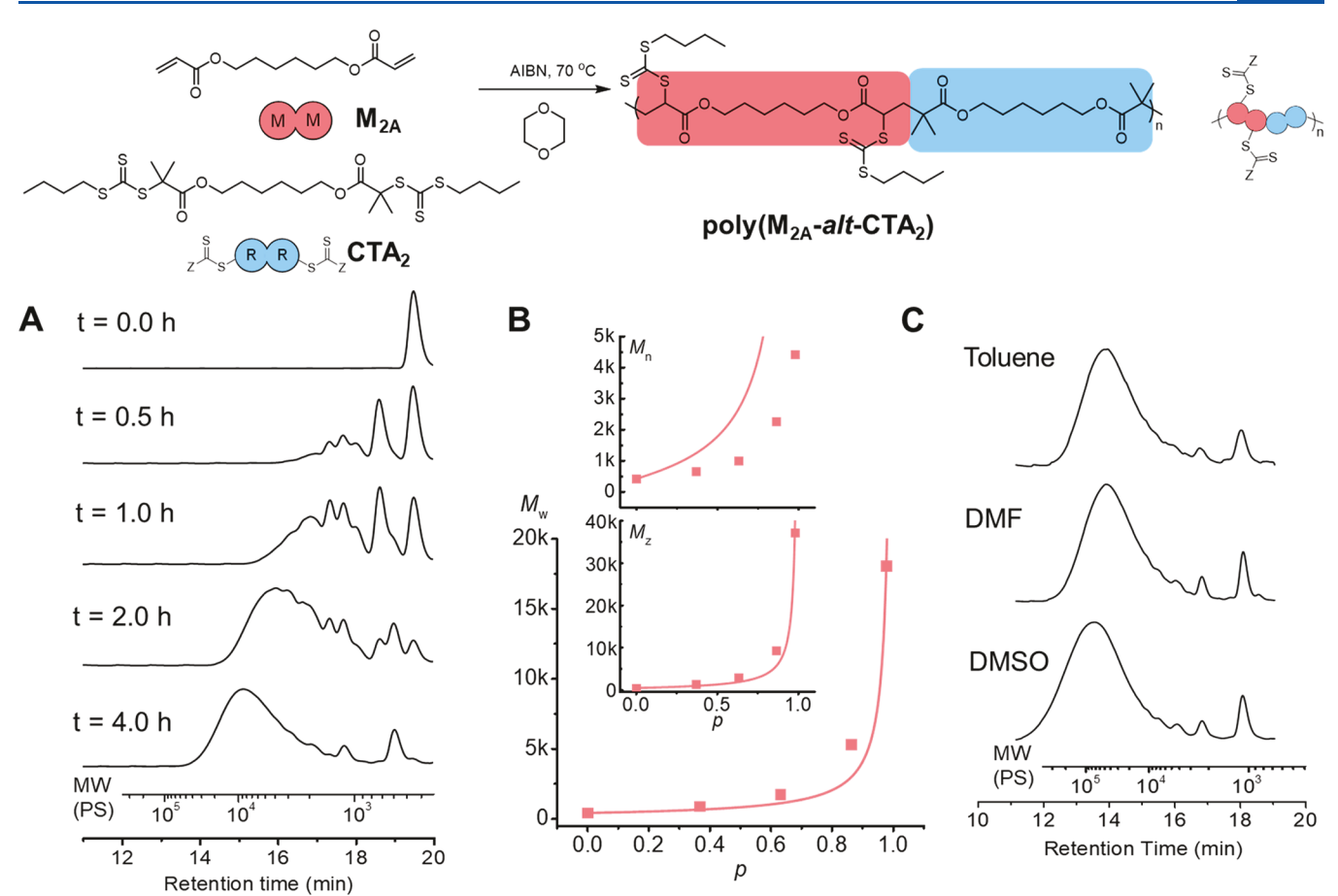


Figure 3. (A) Conventional THF-SEC analysis using polystyrene calibration of RAFT step-growth polymerization of  $M_{2A}$  and  $CTA_2$ . (B) Evolution of the molecular weight averages  $(M_n, M_w \text{ and } M_z)$  determined by SEC analysis and conversion from <sup>1</sup>H NMR, plotted together with theoretical molecular weight averages predicted for step-growth polymerization, which does not consider cyclization. (C) Conventional THF-SEC analysis of poly $(M_{2A}$ -alt-CTA<sub>2</sub>) made in toluene, DMF, or DMSO.

resulted in retarded homopolymerization of BA, as fragmentation is disfavored (Figure S8).

As CTA<sub>1C</sub> demonstrated high SUMI-CTA adduct yields with BA in our model RAFT SUMI study, CTA2 was prepared following our previous report. 14,15 1,6-hexanediol diacrylate  $(M_{2A})$  was chosen as our initial model diacrylate monomer to match the linker length with CTA2. RAFT step-growth polymerization was carried out in 2 M concentration of the monomer functional groups in 1,4-dioxane using stoichiometrically equivalent CTA<sub>2</sub> and initiated using AIBN at 70 °C. The monomer conversion (p) reached 98% after 4 h (Figure 3A), which was determined from <sup>1</sup>H NMR by tracking the disappearance of acrylate peaks (peak m, Figure S9) relative to  $OCH_2$  protons on the Z-group (peaks p and c, Figure S9). Concurrently, the appearance of CH peak next to trithiocarbonate at 4.89 ppm (peak n, Figure S9) and diastereotopic  $CH_2$  peaks at 2.38/2.13 ppm (peaks r/r', Figure S9) is consistent with the bond formation during the polymerization.

Conventional SEC analysis disclosed that the number-average  $(M_{\rm n})$ , weight-average  $(M_{\rm w})$ , and Z-average  $(M_z)$  molecular weight with conversion (p) tracked well with the theoretical molecular weight averages (Figure 3B), <sup>23</sup> indicating polymerization to follow step-growth molecular weight evolution. It is important to note that the  $M_{\rm n}$  is expected to be lower than predicted as cyclization is not considered in the theoretical equation. <sup>23</sup>

We next investigated the effect of changing the concentration of the polymerization ( $[CTA]_0 = 1, 0.5, 0.25 M$ ) with constant initiator concentration ([AIBN]<sub>0</sub> = 50 mM, Figures S11, S13, S15, S17, S19) or equivalence with respect to the CTA ([CTA]<sub>0</sub>/[AIBN]<sub>0</sub> = 40, Figures S12, S14, S16, S18, S20). It is important to note that, in traditional RAFT kinetics, the rate is often dependent on the ratio of CTA to initiator due to retardation, which is typically observed for highly active Zgroups. 19 Here, we found the rate was maintained by keeping the initiator concentration constant, while changing this to keep the equivalence of the initiator constant resulted in a dramatic effect in rate, similar to our early work with maleimidic monomers. 14 It is noteworthy that lower concentrations of [CTA] lead to an increased formation of cyclic species (Figure S17, S18), resulting in much lower  $M_{\rm p}$ (Figure S19, S20), which is an expected feature of step-growth polymerization.<sup>22</sup>

One advantage in traditional RAFT polymerization is the robustness in the use of different solvents. Previously in the case of maleimidic monomers, we found a significant high-molecular-weight shouldering when RAFT step-growth polymerization was carried out in DMF or DMSO; <sup>14</sup> we speculate that this was due to the occurrence of side reactions with maleimides in polar solvents. Pleasingly, RAFT step-growth polymerization of acrylates ( $M_{2A}$  and  $CTA_2$ ) using the same conditions above ( $[M]_0 = 2 M$ ,  $[AIBN]_0 = 0.05 M$ ,  $[M]_0/[CTA]_0 = 1$ , at 70 °C for 4 h) in toluene, DMF, and DMSO all

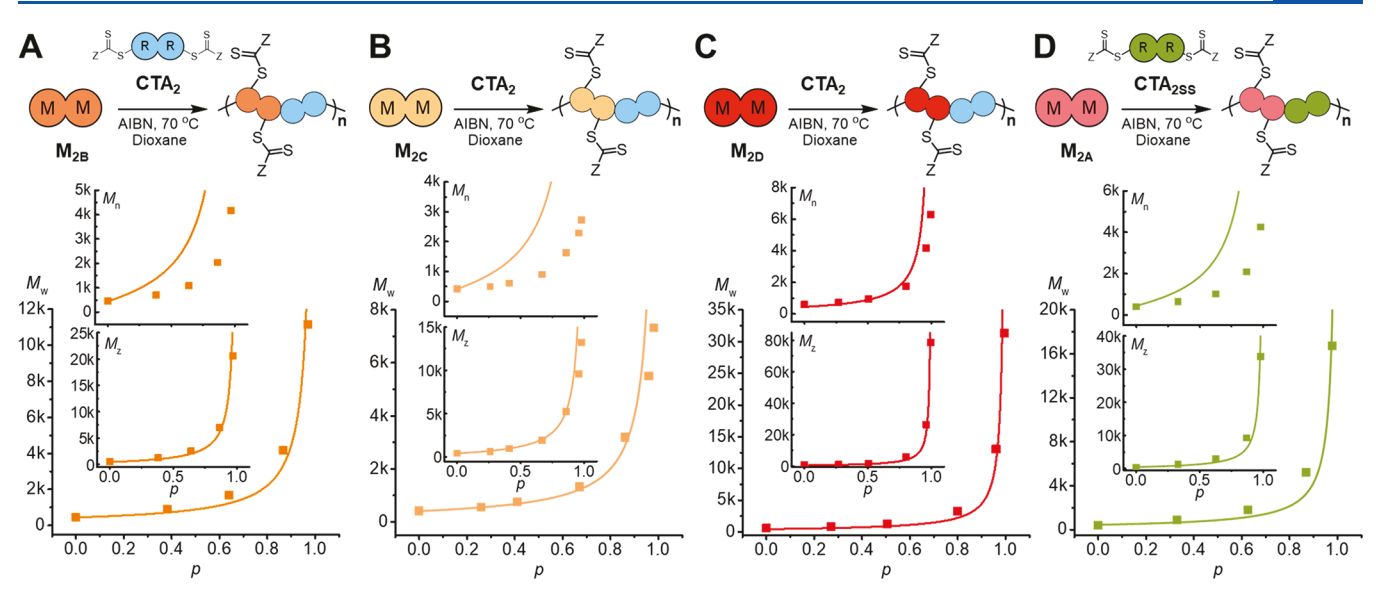


Figure 4. RAFT step-growth polymerization of various diacrylate monomers. The graphs showing evolution of molecular weight averages with conversion of (A) tripropylene glycol diacrylate ( $M_{2B}$ ), (B) neopentyl glycol diacrylate ( $M_{2C}$ ), (C) tricyclo[5.2.1.02,6]decanedimethanol diacrylate ( $M_{2D}$ ), all of which polymerized with CTA<sub>2</sub>, and (D) 1,6-hexanediol diacrylate ( $M_{2A}$ ) polymerized with disulfide tethered CTA (CTA<sub>2SS</sub>).

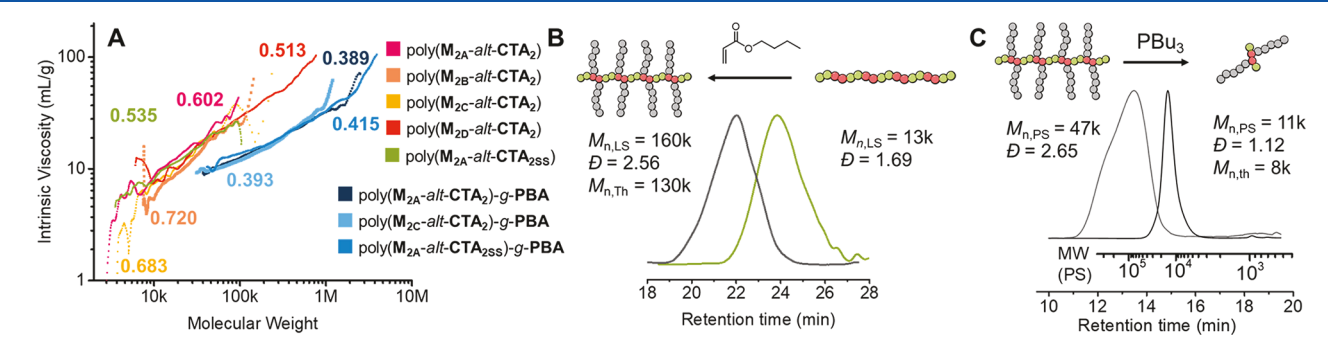


Figure 5. (A) Mark—Houwink plot, the slope is determined from linear regression across the same range of data points used in the molecular weight analysis (red-line in Figures S37—S39). (B) LS-SEC analysis of  $p(M_{2A}$ -alt-CTA<sub>2SS</sub>) and  $p(M_{2A}$ -alt-CTA<sub>2SS</sub>)-g-PBA. The  $M_{n,LS}$  of the linear backbone is used to calculate the expected  $M_{n,th}$  of the graft copolymer. (C) Conventional SEC analysis of  $p(M_{2A}$ -alt-CTA<sub>2SS</sub>)-g-PBA before and after degradation with PBu<sub>3</sub>.

successfully proceeded (Figure 3C, Figures S22–S25), with experimental molecular weight averages tracking well with theoretical values (Figure S26). Interestingly, macro-phase separation had occurred during the polymerization in DMSO (Figure S21), which resulted in apparent autoacceleration in rate (Figure S26).

We next screened various commercially available diacrylate monomers ( $M_{2B-D}$ , Figure 1C) to prepare a library of polymer backbones (Figure 4). Pleasingly, each reaction reached high p (Figures S27–S30) under the same reaction conditions and maintained step-growth molecular weight evolution (Figure 4). In all cases, low-molecular-weight cyclic species were removed upon precipitation, yielding the desired polymer structures. Furthermore, Mark–Houwink analysis was carried out by logarithmic plots of intrinsic viscosity as a function of molecular weight (Figure 5A). Typically, the exponent parameter,  $\alpha$ , which describes conformation of polymers in dilute solution, is in the range of 0–0.5 and 0.5–0.7 for branched and linear polymers, respectively. Indeed, our RAFT step-growth polymers reveal exponent parameters of 0.5–0.72 (Figure 5A), consistent for linear polymers.

A key benefit of step-growth polymerization is the ability to incorporate functionality into the polymer backbone. Pre-

viously we have demonstrated this through bifunctional monomer incorporating silyl ether; <sup>14</sup> here we show an alternative entry of inserting functionality through the bifunctional CTA. This was successfully demonstrated using disulfide tethered bifunctional CTA (CTA<sub>2SS'</sub>, Figure 1C) (Figure 4D, Figures S30, S31). Indeed, RAFT step-growth polymerization with M<sub>2A</sub> and CTA<sub>2SS</sub> proceeded with the expected molecular weight evolution (Figure 4D). As there is vast selection of commercially available diacrylate monomers, shifting the synthetic efforts to preparing functional CTAs should be the future focus.

One key advantage of RAFT step-growth polymers is facile preparation of molecular brush polymers by directly grafting from the backbone. Here we demonstrate molecular brush synthesis with our acrylic step-growth backbone, using BA as a model monomer to graft side chains (Figure 5B). The conversion of BA was determined by H NMR analysis, by following the disappearance vinyl protons at 5.70 ppm with respect to  $CH_3$  at 0.93 ppm (Figures S34–S36). Indeed, the absolute  $M_n$  of the brush polymer, determined by SEC with light scattering, is consistent with the calculated value from the absolute  $M_n$  of the linear backbone (Figure 5B, Figures S37–S39). Additionally, Mark–Houwink plots of the resulting

brushes confirms changes in chain confirmation, as the  $\alpha$  value dramatically decreases, suggesting a transition from linear to denser branched conformation in solution (Figure 5, Figure S40).

Finally, to highlight the benefit of versatility of the polymer backbone made with our methodology, we demonstrate cleavage of the disulfide units along the molecular brush polymers made with poly(M<sub>2A</sub>-alt-CTA<sub>2SS</sub>). Using butanol as the protic solvent, we introduced stochiometric equivalence of tributyl phosphine with respect to disulfide (Figure 5C, Figure S41). Remarkably, after 1 h of introducing the reducing agent, SEC analysis revealed unimolecular species with narrow molecular weight distribution that is close to the expected molecular weight of 2 polymeric side chains (Figure 5C, Figure S41). Such ease of incorporation of degradable functionalities into the polymer backbone opens up RAFT step-growth to applications where degradability is desired such as drug delivery and tissue engineering.<sup>25</sup>

In summary, we successfully demonstrated RAFT step-growth polymerization with diacrylate monomers, expanding the accessibility and potential utility of this new RAFT step-growth method. Further, incorporation of functionality in the polymer backbone can now be achieved via embedding such functionality in the bifunctional CTA. Together with earlier reports, 14–16 these new results demonstrate that RAFT step-growth polymerization is a robust method to prepare a variety of functional linear and brush polymers.

#### ASSOCIATED CONTENT

#### Supporting Information

The Supporting Information is available free of charge at https://pubs.acs.org/doi/10.1021/acsmacrolett.2c00476.

Experimental procedures, Figures S1-S41, and Tables S1-S10 (PDF)

#### AUTHOR INFORMATION

#### **Corresponding Authors**

Joji Tanaka — Department of Chemistry, University of North Carolina, Chapel Hill, North Carolina 27599, United States; Occid.org/0000-0002-2134-8079; Email: joji@email.unc.edu

Wei You — Department of Chemistry, University of North Carolina, Chapel Hill, North Carolina 27599, United States; orcid.org/0000-0003-0354-1948; Email: wyou@ unc.edu

#### Authors

Noel E. Archer – Department of Chemistry, University of North Carolina, Chapel Hill, North Carolina 27599, United States

Parker T. Boeck — Department of Chemistry, University of North Carolina, Chapel Hill, North Carolina 27599, United States

Yasmin Ajirniar — Department of Chemistry, University of North Carolina, Chapel Hill, North Carolina 27599, United States

Complete contact information is available at: https://pubs.acs.org/10.1021/acsmacrolett.2c00476

#### **Author Contributions**

CRediT: **Noel Archer** data curation (equal), formal analysis (equal), investigation (lead), writing-original draft (lead), writing-review & editing (supporting).

#### **Notes**

The authors declare the following competing financial interest(s): J.T. and W.Y. are named inventors on provisional patent application described in this work.

#### ACKNOWLEDGMENTS

This work was financially supported by the National Science Foundation (NSF) under Award CHE-2108670. Bruker AVANCE III Nanobay 400 MHz NMR Spectrometer was supported by the National Science Foundation under Grant No. CHE-0922858. Authors thank Dr. Marc A. ter Horst and Dr. Andrew Camp from University of North Carolina's Department of Chemistry NMR Core Laboratory for the use of their NMR spectrometers; Dr. Sue Mecham and Dr. Sally Lewis for THF-SEC instrumental training.

#### REFERENCES

- (1) Chiefari, J.; Chong, Y. K.; Ercole, F.; Krstina, J.; Jeffery, J.; Le, T. P. T.; Mayadunne, R. T. A.; Meijs, G. F.; Moad, C. L.; Moad, G.; Rizzardo, E.; Thang, S. H. Living Free-Radical Polymerization by Reversible Addition—Fragmentation Chain Transfer: The RAFT Process. *Macromolecules* 1998, 31 (16), 5559—5562.
- (2) Moad, G.; Rizzardo, E. A 20th anniversary perspective on the life of RAFT (RAFT coming of age). *Polym. Int.* **2020**, *69* (8), *658*–661.
- (3) Moad, G.; Rizzardo, E.; Thang, S. H. Living Radical Polymerization by the RAFT Process A Third Update. *Aust. J. Chem.* **2012**, *65* (8), 985–1076.
- (4) Corrigan, N.; Jung, K.; Moad, G.; Hawker, C. J.; Matyjaszewski, K.; Boyer, C. Reversible-deactivation radical polymerization (Controlled/living radical polymerization): From discovery to materials design and applications. *Prog. Polym. Sci.* **2020**, *111*, 101311.
- (5) Perrier, S. 50th Anniversary Perspective: RAFT Polymerization—A User Guide. *Macromolecules* **2017**, *50* (19), 7433–7447.
- (6) Moad, G. RAFT polymerization to form stimuli-responsive polymers. *Polym. Chem.* **2017**, 8 (1), 177–219.
- (7) Rogers, M. E. L., Timothy, E. Synthetic methods in step-growth polymers; John Wiley and Sons: New York, 2003.
- (8) McLeary, J. B.; McKenzie, J. M.; Tonge, M. P.; Sanderson, R. D.; Klumperman, B. Initialisation in RAFT-mediated polymerisation of methyl acrylate. *Chem. Commun.* **2004**, No. 17, 1950–1951.
- (9) McLeary, J. B.; Tonge, M. P.; Klumperman, B. A Mechanistic Interpretation of Initialization Processes in RAFT-Mediated Polymerization. *Macromol. Rapid Commun.* **2006**, 27 (15), 1233–1240.
- (10) McLeary, J. B.; Calitz, F. M.; McKenzie, J. M.; Tonge, M. P.; Sanderson, R. D.; Klumperman, B. A 1H NMR Investigation of Reversible Addition—Fragmentation Chain Transfer Polymerization Kinetics and Mechanisms. Initialization with Different Initiating and Leaving Groups. *Macromolecules* **2005**, *38* (8), 3151–3161.
- (11) McLeary, J. B.; Calitz, F. M.; McKenzie, J. M.; Tonge, M. P.; Sanderson, R. D.; Klumperman, B. Beyond Inhibition: A 1H NMR Investigation of the Early Kinetics of RAFT-Mediated Polymerization with the Same Initiating and Leaving Groups. *Macromolecules* **2004**, 37 (7), 2383–2394.
- (12) Chen, M.; Ghiggino, K. P.; Mau, A. W. H.; Rizzardo, E.; Sasse, W. H. F.; Thang, S. H.; Wilson, G. J. Synthesis of Functionalized RAFT Agents for Light Harvesting Macromolecules. *Macromolecules* **2004**, 37 (15), 5479–5481.
- (13) Chen, M.; Ghiggino, K. P.; Rizzardo, E.; Thang, S. H.; Wilson, G. J. Controlled synthesis of luminescent polymers using a bis-dithiobenzoate RAFT agent. *Chem. Commun.* **2008**, No. 9, 1112–1114.

- (14) Tanaka, J.; Archer, N. E.; Grant, M. J.; You, W. Reversible-Addition Fragmentation Chain Transfer Step-Growth Polymerization. *J. Am. Chem. Soc.* **2021**, *143* (39), 15918–15923.
- (15) Boeck, P.; Archer, N.; Tanaka, J.; You, W. Reversible Addition-Fragmentation Chain Transfer Step-Growth Polymerization with Commercially Available Inexpensive Bis-Maleimides. *Polym. Chem.* **2022**. *13*, 2589–2594.
- (16) Li, Z.; Li, J.; Pan, X.; Zhang, Z.; Zhu, J. Catalyst-Free, Visible-Light-Induced Step-Growth Polymerization by a Photo-RAFT Single-Unit Monomer Insertion Reaction. *ACS Macro Lett.* **2022**, *11*, 230–235.
- (17) Haven, J. J.; Hendrikx, M.; Junkers, T.; Leenaers, P. J.; Tsompanoglou, T.; Boyer, C.; Xu, J.; Postma, A.; Moad, G. Elements of RAFT Navigation. In *Reversible Deactivation Radical Polymerization: Mechanisms and Synthetic Methodologies*; Matyjaszewski, K., Gao, H., Sumerlin, B. S., Tsarevsky, N. V., Eds.; American Chemical Society: 2018; Vol. 1284, pp 77–103.
- (18) Chen, M.; Häussler, M.; Moad, G.; Rizzardo, E. Block copolymers containing organic semiconductor segments by RAFT polymerization. *Organic & Biomolecular Chemistry* **2011**, 9 (17), 6111–6119.
- (19) Bradford, K. G. E.; Petit, L. M.; Whitfield, R.; Anastasaki, A.; Barner-Kowollik, C.; Konkolewicz, D. Ubiquitous Nature of Rate Retardation in Reversible Addition—Fragmentation Chain Transfer Polymerization. J. Am. Chem. Soc. 2021, 143 (42), 17769—17777.
- (20) Houshyar, S.; Keddie, D. J.; Moad, G.; Mulder, R. J.; Saubern, S.; Tsanaktsidis, J. The scope for synthesis of macro-RAFT agents by sequential insertion of single monomer units. *Polym. Chem.* **2012**, *3* (7), 1879–1889.
- (21) Zhou, Y.; Zhang, Z.; Reese, C. M.; Patton, D. L.; Xu, J.; Boyer, C.; Postma, A.; Moad, G. Selective and Rapid Light-Induced RAFT Single Unit Monomer Insertion in Aqueous Solution. *Macromol. Rapid Commun.* **2020**, *41* (1), 1900478.
- (22) Keddie, D. J. A guide to the synthesis of block copolymers using reversible-addition fragmentation chain transfer (RAFT) polymerization. *Chem. Soc. Rev.* **2014**, *43* (2), 496–505.
- (23) Flory, P. J. Molecular Size Distribution in Linear Condensation Polymers. J. Am. Chem. Soc. 1936, 58, 1877–1885.
- (24) Kricheldorf, H. R. The Role of Self-Dilution in Step-Growth Polymerizations. *Macromol. Rapid Commun.* **2008**, 29 (21), 1695–1704.
- (25) Käpylä, E.; Delgado, S. M.; Kasko, A. M. Shape-Changing Photodegradable Hydrogels for Dynamic 3D Cell Culture. *ACS Appl. Mater. Interfaces* **2016**, 8 (28), 17885–17893.

### **□** Recommended by ACS

# **Ubiquitous Nature of Rate Retardation in Reversible Addition–Fragmentation Chain Transfer Polymerization**

Kate G. E. Bradford, Dominik Konkolewicz, et al.

OCTOBER 18, 2021

JOURNAL OF THE AMERICAN CHEMICAL SOCIETY

READ 🗹

# Stereochemistry-Induced Discrimination in Reaction Kinetics of Photo-RAFT Initialization

Lei Zhang, Jiangtao Xu, et al.

MARCH 22, 2022

MACROMOLECULES

READ 🗹

#### Solvent Effects in Grafting-through Ring-Opening Metathesis Polymerization

Sarah E. Blosch, John B. Matson, et al.

APRIL 22, 2022

MACROMOLECULES

READ 🗹

#### Manipulating Molecular Weight Distributions via "Locked-Unlocked" Anionic Polymerization

Cun Li, Hongwei Ma, et al.

SEPTEMBER 13, 2021

MACROMOLECULES

READ **C** 

Get More Suggestions >